HighNoon Delivery Report

Title	Report on intercomparison of the relative performance of the three modelling approaches
Work Package Number	WP 2
Delivery number	D 2.4
Relative task(s)	2.9
Organization	USAL
Author	Collins, D.N., Siderius, C.Biemans, H., Rao, S., Wiltshire, A., Franssen, W.H.P.,Kumar, P., Gosain, A. K., M.T.H. van Vliet
Function	WP Leader, Senior scientist
Related to deliverable number(s)	-
Date of completion	26 April 2012
Name Work Package Leader	D.N. Collins
Submission Date	27 April

To complete by the Coordinator

Date of approval by the Coordinator	27 April 2012

Report on intercomparison of the relative performance of the three modelling approaches:

Snowmelt contributions to discharge of the Ganges – A multi-model approach

Report of the FP7 project: HighNoon
Contract number 227087

www.eu-highnoon.org

Summary

Himalayan headwaters supply large quantities of runoff derived from snowmelt and monsoon rainfall to the Ganges river. Actual snowmelt contribution to discharge in the Ganges remains conjectural under both present and future climatic conditions. As snowmelt is likely to be perturbed through climatic warming, four hydrological models, VIC, JULES, LPJmL and SWAT, appropriate for coupling with regional climate models, were used to provide a baseline estimate of snowmelt contribution to flow at seasonal and annual timescales. The models constrain estimates of snowmelt contributions to between 1 and 5% of overall basin runoff. Snowmelt is however significant in spring months, a period in which other sources of runoff are scarce.

This deliverable is based on the paper: Siderius, C.Biemans, H., Rao, S., Wiltshire, A., Franssen, W.H.P.,Kumar, P., Gosain, A. K., M.T.H. van Vliet, Collins, D.N. (2012, under review). Snowmelt contributions to discharge of the Ganges – a multi-model approach. submitted to *Geophysical Research Letters*

1. Introduction

High specific discharges in tributaries draining from Himalayan catchments contribute large quantities of snowmelt- and monsoon-rainfall-derived runoff to the main stem Ganges river. As climate warms, reduced snow accumulation will lead to snowmelt runoff both declining and occurring earlier in spring, a period when water availability from other sources is scarce. Combined with reducing glacier melt [*Fujita and Nuimura*, 2011; *Singh et al.*, 2006], falling groundwater levels [*Rodell et al.*, 2009], uncertain monsoon rainfall [*Christensen et al.*, 2007] and continuing population growth, sustainability of water resources for millions of people in the Ganges basin is questionable [*Immerzeel et al.*, 2010; *Moors et al.*, 2011].

Actual snowmelt contribution to discharge in the Ganges remains conjectural under both present and future climatic conditions. Estimates of snow- and icemelt contributions to total runoff in the Ganges range from almost 0% to 70% [*Barnett et al.*, 2005; *Immerzeel et al.*, 2010; *Kaser et al.*, 2010; *Seidel et al.*, 2000]. In the absence of field data, *Seidel et al.* [2000] estimated the snowmelt proportion of total annual runoff in the Ganges as 9%, using an empirical degree day snowmelt-runoff model. *Immerzeel et al.* [2010] used a combination of the same snowmelt model coupled with a global hydrological model to confirm 10%, 40% of which was derived from icemelt and 60% from snowmelt. Using a basic glacier mass budget model *Kaser et al.*[2010] estimated a maximum icemelt contribution of 14% in June in Ganges headwater catchments, rapidly reducing to almost 0% downstream. However, a snowmelt-contribution to runoff as high as 70% in summer has also been quoted [*Barnett et al.*, 2005]. Of the above models, only that of [*Seidel et al.*, 2000] was validated against measured discharge data from the Ganges basin and that for only a single station.

This study aims to quantify and clarify current temporal and spatial contributions of snowmelt[1] to runoff at the scale of the Ganges basin, with a view to setting baseline contributions against which future climate change impacts on thermally-controlled components of runoff can be compared. The intention was to use validated models, both suited to the scale and data scarcity of the Ganges basin and appropriate for forcing with high resolution dynamically based regional climate models. Four such hydrological models (VIC [*Liang et al.*, 1994], JULES [*Best et al.*, 2011], LPJmL [*Gerten et al.*, 2004] and SWAT [*Arnold and Fohrer*, 2005]) were used to estimate proportions of flow in the Ganges, arising from snowmelt along the Himalayan arc. The models contained differing representations of snow accumulation and melt, but where forced with the same meteorological data.

2. Materials and methods

Four sub-catchments were selected (Figure 1) to characterize conditions along the Himalaya arc, together with the main stem Ganges basin above the Farakka dam. Monthly discharge data were acquired from the Global Runoff Data Centre [*GRDC*, 2011] except for Tehri (WADIA Institute) for validation of the four large-scale catchment models. The models use differing snowmelt routines, between simple degree day and full energy balance approaches,

[1] Snow melt as used in this paper represents the seasonal melt from snow on both soil and glacier as well as melt from inter-annual variations in the snowpack over the 1971-2000 period. In reality this component will partly have converted into ice. It does not included the deglaciation discharge dividend, e.g. the amount of extra melt which permanently reduces the glacier volume over the period considered.

and varying representations of topography from single mean grid-cell elevations or division into (up to 25) elevation bands. Model validation also involved snow cover over the Himalaya region derived from MODIS imagery (MOD10A2; [*Hall et al.*, 2006]) with monthly average resolution (see supplement for model and subcatchment characteristics and snow cover validation).

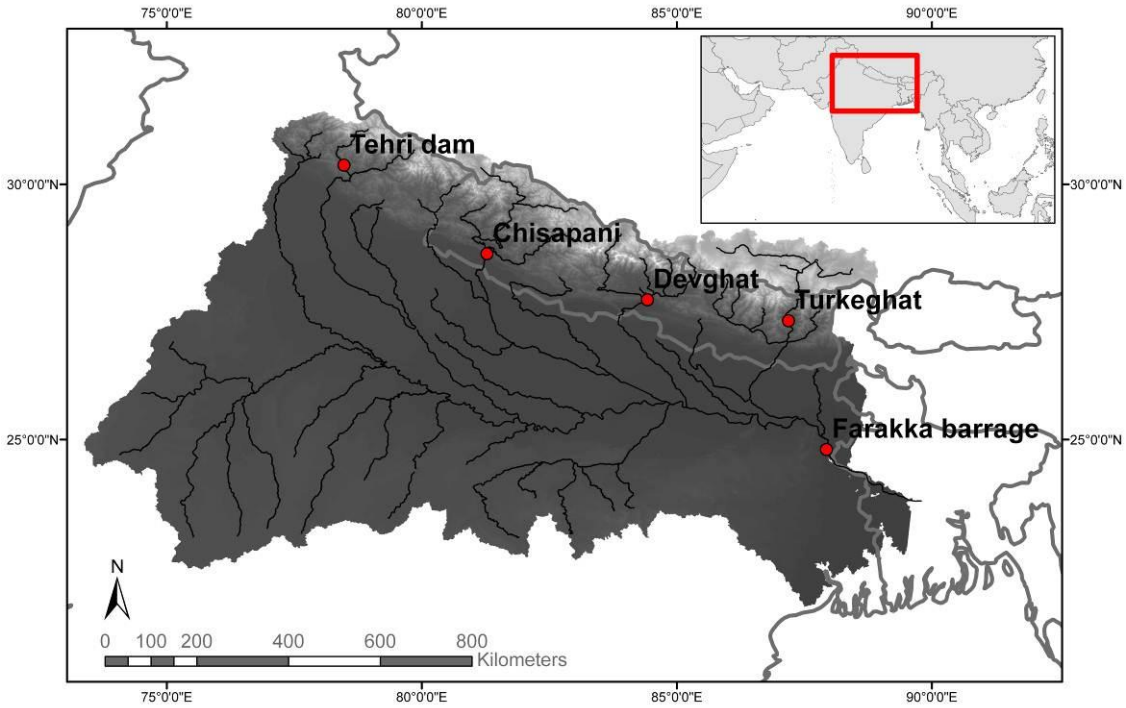

Figure 1. Ganges basin and selected locations for discharge validation. Elevation in grey shades.

In the models, runoff is generated from water that has percolated through the soil column. Such water arises from both rainfall and snowmelt, components which are not treated separately in the models. Runoff arising from snowmelt (in mm month^{-1}) was calculated for each gridcell and month *i*, by:

$$Runoff_{snowmelt,i} = \min\left\{ Runoff_{total,i} * \left[\frac{Melt_i}{Rain_i + Melt_i} \right], Melt_i \right\} \quad \{1\}$$

Overall snowmelt contribution to runoff per grid cell (0.5 degree resolution) in the Ganges basin was averaged over the period 1971-2000 creating an ensemble of all four models. The subcatchment-based output of SWAT was scaled back to the grid size of the other three models using area averaging. Both snowmelt runoff and total runoff were routed downstream using the STN routing scheme [*Vörösmarty et al.*, 2000]. To visualize snowmelt contributions decreasing along the river stretches downstream, snowmelt runoff and total runoff were averaged at equal distances from the uppermost grid cell for the seven most important tributaries draining from the Himalaya (see supplement).

3. Results

For all stations the models show discharge patterns with discharge peaking in July-August (figure 2). For the western Himalayan subcatchment (Karnali above Chisipani) there is good correspondence between all the models and the observed runoff in terms of rise, maximum and decline of the discharge peak pattern. Broadly similar model performances for the central subcatchment (Narayani above Devghat), however, produce peaks in runoff a month ahead of the observed, with SWAT underestimating the maximum most. For the eastern subcatchment, Arun above Turkeghat, all models clearly overestimate runoff. Most likely this is caused by overestimation in precipitation model input data in the upper Arun catchment, on the dry Tibetan plateau (see also supplement).

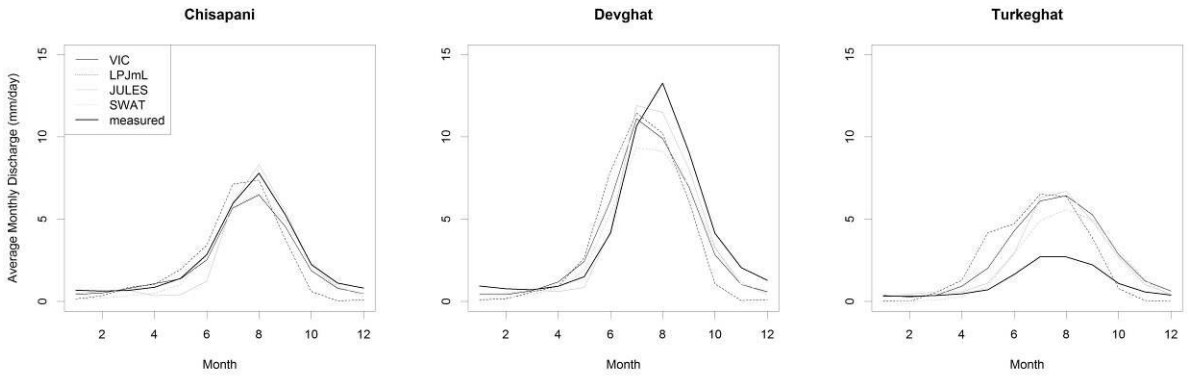

Figure 2. Modeled and measured monthly average discharge for the upstream location from west to east (only those stations are presented for which measured and modelled periods at least partly overlap. Chisipani and Devghat measured 1971-1993; Turkeghat measured 1976-1986; all models 1971-2000)

Discharge for the full Ganges basin above Farakka (not shown) is overestimated (between 37% and 82%) by all four models. For a large part this can be explained by abstraction for irrigation, not included in any of the current models. For the upstream station at Tehri (not shown) discharges are overestimated by all models (between 16% and 127%). The area upstream of Tehri is covered by only one gridcell in the models, making model output sensitive to schematization and input biases.

Snowmelt contributions to runoff vary between the four models for all five stations (table 1). Absence of elevation bands in JULES and LPJmL is reflected in snowmelt contributions to runoff being low. SWAT includes a schematization into10 elevation bands, but has a lower snow/rain split at elevation compared to VIC and LPJmL and is therefore generating less snowfall. JULES is different in that the snow/rain split is prescribed in the WATCH forcing, which resulted in an even lower amount of snow input into the model. VIC, with its 25 elevation bands and internal calculation of snow/rain split, follows the seasonal pattern of snow cover best and calculates the highest contribution of snowmelt to runoff. The models suggest that runoff at all five stations (except maybe SWAT at Tehri), irrespective of catchment elevation, is monsoon-rainfall-dominated. At 16%, VIC gives a snowmelt

contribution for the Karnali sub-catchment above Chisapani not dissimilar to the 20% estimated by *Bookhagen and Burbank* [2010].

Table 1. snowmelt contribution to discharge (in %) for the different models for the different stations

		LPJmL	*JULES*	*SWAT*	*VIC*
Annual contribution of snowmelt runoff to total discharge (%)	Chispani	11	4	11	16
	Devghat	8	2	7	13
	Turkeghat	15	4	10	30
	Tehri	2	8	49	15
	Farakka	3	1	4	5
March-April-May contribution of snowmelt runoff to total discharge (%)	Farakka	38	12	13	21

Overall, on an annual basis, for the Ganges basin above Farakka as a whole, snowmelt contributions to runoff are between 1% and 5%. Snowmelt contribution to runoff declines rapidly down basin, from annual average contributions between 10% and 30% in upstream reaches to between 4% and 14% by 250 km downstream (figure 3) and is reduced to almost 0% by 750 km, on confluence of monsoon-fed tributaries from the south. Downstream from 1500km, tributaries from Nepal, e.g. Gandak and Kosi rivers, slightly increase overall snowmelt contribution to runoff.

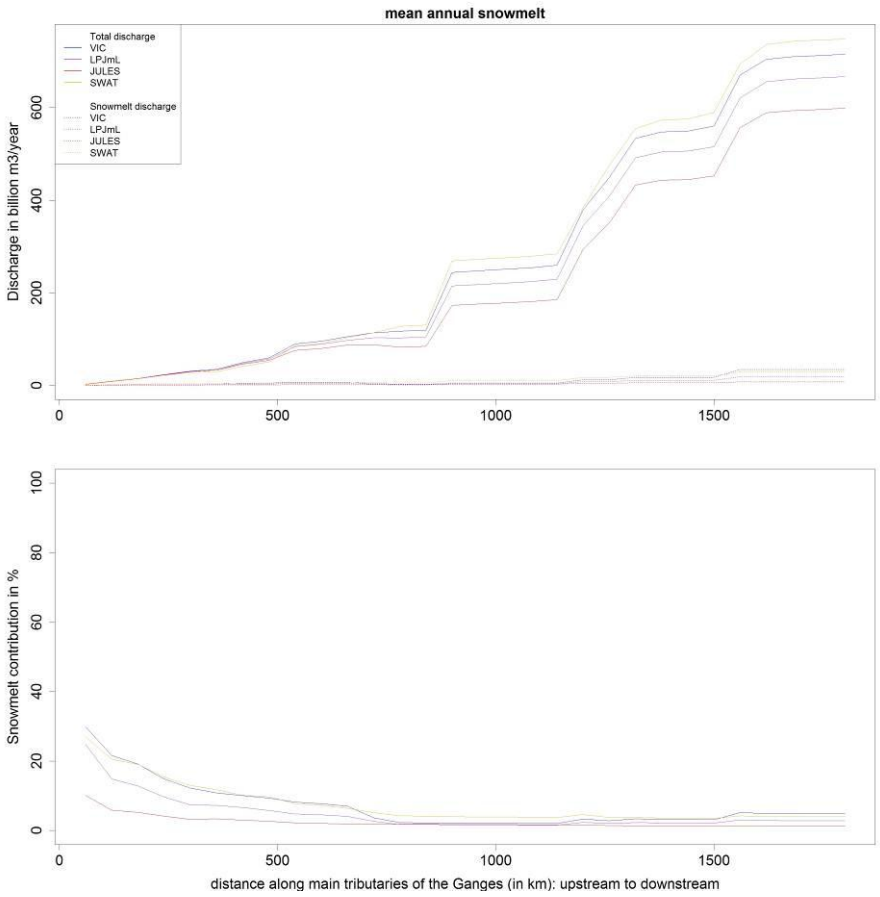

Figure 3. Average annual total discharge and snowmelt discharge (top) and the contribution in % (bottom) along the main stem of the Ganges river (from the most upstream gridcell of the Upper Ganga to Farakka) for the different models for the period 1971-2000

Seasonally, there is considerable variation in snowmelt contributions to total runoff (Figure 4). During the spring months March through May (MAM), snowmelt contributes large proportions of total flow, reaching far downstream as there is no other source of runoff. Estimates of average contributions of snowmelt to total runoff in MAM range from 39% to 77% upstream, remaining between 16% and 51% to 850 km downstream. Even as far as Farakka, snowmelt contribution to total runoff during this season varies between 12% and 38% dependent on the model used. In summer, runoff is totally dominated by monsoon rainfall. During winter, both snowmelt contribution and total runoff are low because of limited rainfall and snowmelt being suppressed by low temperatures in mountainous areas.

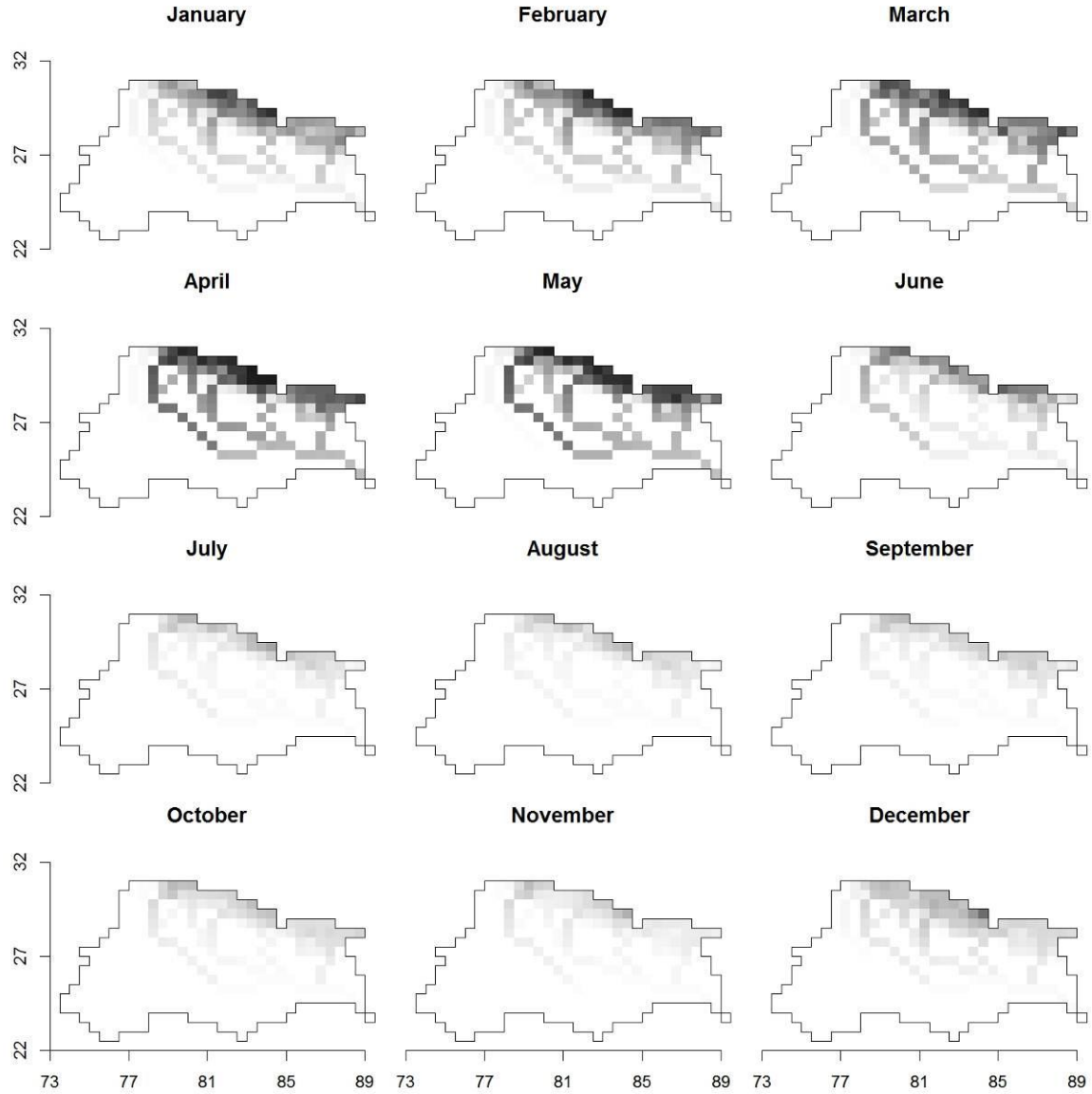

Figure 4. Snowmelt contribution to runoff (%)in the Ganges basin, averaged over the different months for the whole basin, based on an ensemble of VIC, LPJmL, JULES and SWAT model runs for the period 1971-2000 (white = 0% , black = 100%)

4. Discussion and conclusions

Use of the four models in this study has allowed estimates of snowmelt contributions to runoff at the scale of the Ganges basin to be constrained. Values between approximately 1% and 5% can be taken as indicative of actual contributions of snowmelt to overall runoff. JULES and LPJmL may be underestimating total snowmelt contribution as snow availability for melting is exhausted later in the season. Three of the models represent well both onset of melt and the spring snowmelt peak

Both amount and timing of snow accumulation and melt as produced by the models are greatly influenced by the way they handle elevation. In snowmelt modeling, the zero degree isotherm in the atmosphere is a critical threshold partitioning snow accumulation and melt. Use of average gridcell temperatures over wide elevation ranges fails to accurately represent both timing and quantity of snowmelt. This can partly be compensated for by introduction of elevation bands. In the elevation band based VIC and SWAT models a larger part of the Ganges basin was covered by permanent snow and the annual snowmelt contribution to runoff was higher than in the average elevation JULES and LPJmL models. Use of elevation bands captures heterogeneity and allows the application of temperature lapse rates to model.

Conversion of snowmelt to runoff in the models is greatly influenced by the schematization of the soil in combination with the lack of distinction between runoff from glaciers and runoff from seasonal snow (see also supplement). In reality, melt from glaciers mostly directly enters a surface water stream with minimal loss to groundwater recharge or evapotranspiration. This in contrast to melt from seasonal snowmelt, which might enter the soil. In none of the models can this distinction be made and all melt enters the soil. As shown for the VIC model, use of a global soil dataset with an overestimated soil thickness in the Himalaya can lead to delay in runoff and overestimation of losses.

The discussion on the relative merits of Degree-Day (DD) and Energy-Balance (EB) algorithm is on-going in literature (e,g . Gudmundsson et al. 2009). This study provides no evidence that one type of model is performing better than another and the snowmelt algorithm formulation is likely to be a second order effect in comparison to e.g. the generation of snowfall, either prescribed from the forcing data (as in JULES) or internally calculated, and the representation of elevation. However, in general DD models are less likely to be able to capture the melt-processes in these regions of high topography then EB models, particularly due to their inability to capture non-temperature driven ablation such as net radiation and sublimation, expected to be an important component of the mass balance at high elevations.

During the dry season and onset of the monsoon season, when rising temperatures are accompanied by snowmelt from the Himalayas, agriculture relies on additional irrigation from surface and groundwater. Although being only a relatively low proportion of the annual flow, snowmelt nonetheless sustains agricultural production during these vital months in both the mountainous regions as well as in the irrigated areas of the Indo-Gangetic plain. As climate warms this is of considerable importance for a sustainable agriculture.

Acknowledgements
This work has been supported by the HighNoon project, funded by the European Commission Framework Programme 7 under Grant Nr. 227087. A. Wiltshire was partly supported by the Joint DECC/Defra Met Office Hadley Centre Climate Programme (GA01101).

References
Arnold, J. G., and N. Fohrer (2005), SWAT2000: current capabilities and research opportunities in applied watershed modelling, *Hydrological Processes*, *19*(3), 563-572.
Barnett, T. P., J. C. Adam, and D. P. Lettenmaier (2005), Potential impacts of a warming climate on water availability in snow-dominated regions, *Nature*, *438*(7066), 303-309.
Best, M. J., et al. (2011), The Joint UK Land Environment Simulator (JULES), Model description – Part 1: Energy and water fluxes, *GeoScientific Model Development*, *4*(1), 595-640.
Bookhagen, B., and D. W. Burbank (2010), Toward a complete Himalayan hydrological budget: Spatiotemporal distribution of snowmelt and rainfall and their impact on river discharge, *Journal of Geophysical Research*, *115*(F3), 1-25.
Christensen, J. H., et al. (2007), Regional Climate Projections, in *IPCC, 2007: Climate Change 2007: The Physical Science Basis. Contribution of Working Group I to the Fourth Assessment Report of the Intergovernmental Panel on Climate Change*, edited by S. Solomon, D. Qin, M. Manning, Z. Chen, M. Marquis, K. B. Averyt, M. Tignor and H. L. Miller, Cambridge University Press, Cambridge.
Fujita, K., and T. Nuimura (2011), Spatially heterogeneous wastage of Himalayan glaciers, *Proceedings of the National Academy of Sciences*, *108*(34), 14011-14014.
Gerten, D., S. Schaphoff, U. Haberlandt, W. Lucht, and S. Sitch (2004), Terrestrial vegetation and water balance - Hydrological evaluation of a dynamic global vegetation model, *Journal of Hydrology*, *286*(1-4), 249-270.
GRDC (2011), Long-Term Mean Monthly Discharges and Annual Characteristics of GRDC Station / Global Runoff Data Centre, edited, Federal Institute of Hydrology (BfG), Koblenz.
Guðmundsson S, Björnsson H, Pálsson F, Haraldsson HH. 2009. Comparison of energy balance and degree-day models of summer ablation on the Langjökull ice cap, SW-Iceland. *Jökull*, 59: 1–18.
Hall, D. K., G. A. Riggs, and V. V. Salomonson (2006), MODIS/Terra Snow Cover 8-day L3 Global 500m Grid V005, jan 2000 - present, updated weekly, edited, National Snow and Ice Data Center, Boulder, Colorado USA.
Immerzeel, W. W., L. P. H. van Beek, and M. F. P. Bierkens (2010), Climate Change Will Affect the Asian Water Towers, *Science*, *328*(5984), 1382-1385.
Kaser, G., M. Grosshauser, and B. Marzeion (2010), Contribution potential of glaciers to water availability in different climate regimes, *Proceedings of the National Academy of Sciences*, *107*(47), 20223-20227.
Liang, X., D. P. Lettenmaier, E. F. Wood, and S. J. Burges (1994), A Simple hydrologically Based Model of Land Surface Water and Energy Fluxes for GSMs, *Journal of Geophysical Research*, *99*(D7), 415-428.
Moors, E. J., et al. (2011), Adaptation to changing water resources in the Ganges basin, northern India, *Environmental Science & Policy*, *14*(7), 758-769.

Rodell, M., I. Velicogna, and J. S. Famiglietti (2009), Satellite-based estimates of groundwater depletion in India, *Nature*, *460*(7258), 999-1002.
Seidel, K., J. Martinec, and M. F. Baumgartner (2000), Modelling runoff and impact of climate change in large Himalayan basins, in *Integrated Water Resources Management for Sustainable Development II*, edited by R. B. Mehrotra and K. K. S. B. Soni, pp. 1020-1028, National Institute of Hydrology, Roorkee, India.
Singh, P., M. Arora, and N. K. Goel (2006), Effect of climate change on runoff of a glacierized Himalayan basin, *Hydrol. Process.*, *20*(9), 1979-1992.
Vörösmarty, C. J., B. M. Fekete, M. Meybeck, and R. B. Lammers (2000), Global system of rivers: Its role in organizing continental land mass and defining land-to-ocean linkages, *Global Biogeochemical Cycles*, *14*(2), 599-621.

ANNEX I Supplemental material

1 Models

Four large-scale hydrological models, VIC [*Liang et al.*, 1994], JULES [*Best et al.*, 2011; *Clark et al.*, 2011], LPJmL [*Gerten et al.*, 2004; *Rost et al.*, 2008] and SWAT [*Arnold and Fohrer*, 2005] were selected. In a model comparison of eleven models (including JULES, VIC and LPJmL) [Haddeland et al., 2011] found that the degree-day approach in most places resulted in higher Snow Water Equivalent (SWE) values than the energy balance approach both in the winter season and in spring. However, other differentiating factors were identified as well, like the number of snow layers, snow albedo values, and how much liquid water can be retained within the snowpack. The models in this study were chosen in order to cover a range of approaches to snowmelt modeling, from full scale energy balance to degree day approaches, and using simple mean grid-cell elevation or up to 25 elevation bands (table 1).

Table 1. General characteristics and snow module characteristics of the four models used

	LPJmL	**SWAT**	**JULES**	**VIC**
Snowmelt generation	Degree day	Degree day	Full energy balance	Internal energy balance
Elevation bands	1	10	1	25
Structure	Grid (0.5 degrees), daily timestep	Subcatchments (total of 414), daily timestep	Grid (0.5 degrees) Hourly timestep	Grid (0.5 degrees) subdaily timestep
Forcing variables for snow module	Temperature, Precipitation	Temperature, Precipitation	Temperature, Liquid and Solid Precipitation, Downwelling short- and long-wave radiation, Humidity, Windspeed	Minimum and maximum Temperature, Precipitation and Windspeed
Snow- Rainfall split	Internal, based on temperature threshold	Internal, based on temperature threshold	Prescribed in WATCH forcing data	Internal, based on temperature threshold
Snowcharacteristics	None, SWE only	None, SWE only	3 layers prognostic density and snow hydrology	2 layers: density increases with temperature
- Density				
- Albedo	NA	NA	Dynamic	Dynamic
- Coverage	NA	NA	9 subgrid tiles	25 elevation bands
Melt temperature threshold (degree)	0	0	NA	NA
Initial Conditions	Spun-up for 10000 years	SWE estimate based on MODIS snowcover	Spun-up by looping over 1960-1970	Spin-up period from 1958-1970
Period of calculations	1971-2000	1971-2000	1971-2000	1971-2000
Data sources				
- Elevation		GTOPO30	N/A	SRTM (Van Zyl, 2001)
- Land use	Combination of MODIS-derived land cover product and the GLC2000 data set (Ramankutty et al., 2009)	An Irrigated Area Map of the World (Thenkabail et al., 1999)	Global Land Cover Characteristics (version 2) (USGS)	University of Maryland Global Land Cover 1km map (Hansen et al, 2000)
- Soil	FAO digitized Soil map of the world (release1.0) (FAO 1991)	Harmonized World Soil Database (version 1.1)	Harmonised Soils and Wetlands Database (HWSD) (FAO, 2009)	Soil map of the world (FAO, 1995), combined with the World Inventory of Soil Emission Potentials pedon database (Batjes, 1995)

The three models with global coverage (VIC, LPJmL and JULES) were used in their global configuration, with no additional calibration of parameters for the Ganges and subcatchments, except for the soil profile thickness in the Himalayas in VIC. VIC's soil profile of approximately 3m caused an overestimation of rain and snowmelt infiltration and storage, leading to a delayed runoff and increased losses. Therefore, soil profile thickness in the Himalaya (all cells with an elevation of 500m or higher) was reduced to a minimum value of approximately 60 cm. The SWAT model was specifically set-up for the Ganges basin, but its input data on climate, soils and land use is of similar scale and detail to that of the global models. In this study we focused on the present climate conditions using model output for the period 1971-2000.

Overall snowmelt contribution to runoff per grid cell (0.5 degree resolution) in the Ganges basin was averaged creating an ensemble of all four models. The subcatchment-based output of SWAT was scaled back to the grid size of the other three models using area averaging. Both snowmelt runoff and total runoff were routed downstream using the STN routing scheme [*Vörösmarty et al.*, 2000]. To visualize snowmelt contributions decreasing along the river stretch downstream, snowmelt runoff and total runoff were averaged at equal distances from the uppermost grid cell for the seven most important tributaries draining from the Himalaya (Figure 1).

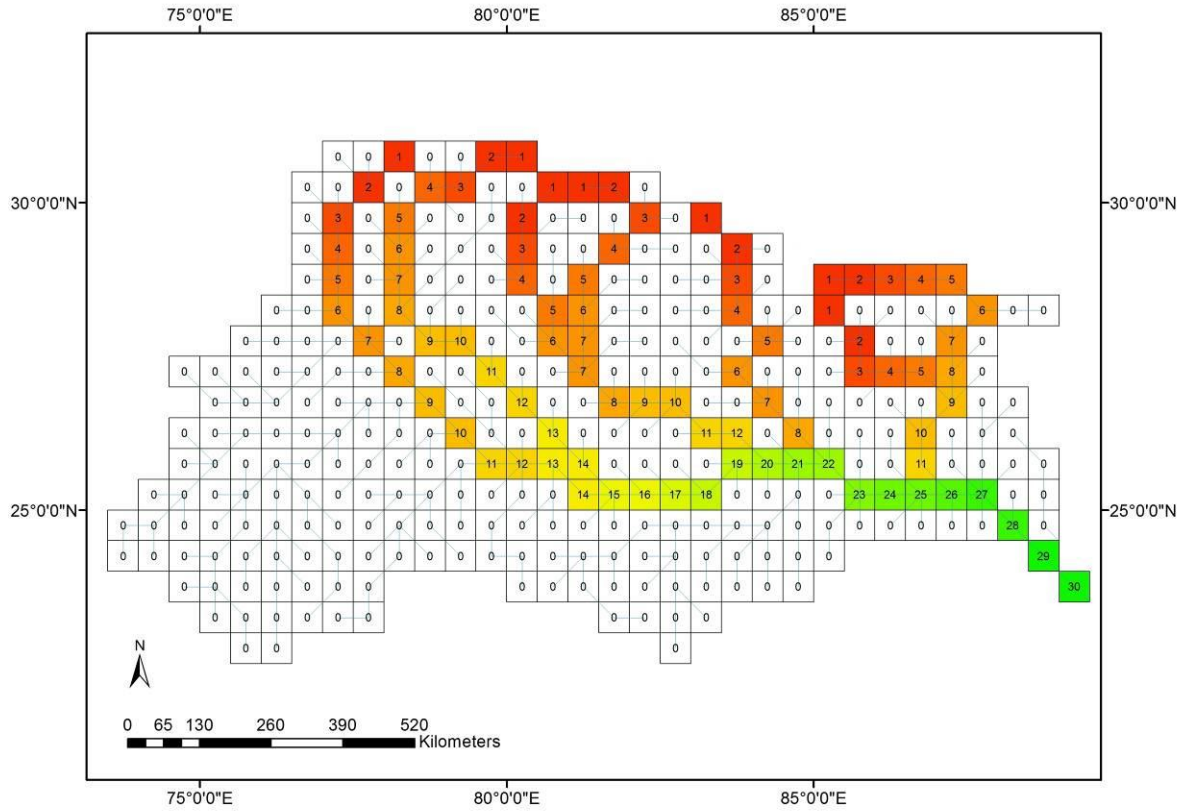

Figure 1. Ganges delineation and river routing network with grid cell numbering representing equal distance to the upstream gridcell for each of the main Himalayan tributaries.

2 WATCH climate forcing data

To force the hydrological models WATCH forcing data (WFD) (developed in the EU FP6 Water and Global Change (WATCH) project) has been used, which is a global gridded (0.5° x 0.5°) sub daily meteorological data set for the period 1958-2001 [*Weedon et al.*, 2010]. WFD was compared for the Ganges region against observed APHRODITE precipitation, a gridded (0.25° x 0.25°) rainfall data set for South Asia [*Yatagai et al.*, 2009]. APHRODITE gridded data has been prepared using rain-gauge observations obtained from meteorological and hydrological stations over the region 60°E-150°E, 0°N-55°N. The yearly cycle of mean daily precipitation of WFD and APHRODITE over the Ganges domain for the period 1971-2000 corresponds well, although daily precipitation in the monsoon season is slightly higher for WFD (correlation between the APHRODITE and WFD data is 0.95 (Pearson's r) for the period 1971-2000) . In addition, WFD precipitation is slightly higher over some locations of the Indo-Gangetic belt, especially on the north-east edge of the Himalaya, compared to APHRODITE values.

3 Model validation

3.1 Snow cover validation

Land surface models have proven to model snow cover accurately [*Parajka et al.*, 2010]. Model validation was conducted using satellite derived snow cover over the Himalaya region from the Moderate Resolution Imaging Spectroradiometer (MODIS) aboard the TERRA satellite, which has a high accuracy in estimating snow cover under cloud free conditions [*Parajka and Blöschl*, 2006]. 8-Day composites with a 500m resolution (MOD10A2; [*Hall et al.*, 2006]) for the period 2000 – 2010 were used. A comparison was made for long-term monthly average snow cover. As LPJmL and JULES do not explicitly model snow cover, but snow water equivalent (SWE) over complete grid cells, the volumes were translated to snow cover using the area-volume relationship for mountainous regions by [*Roesch et al.*, 2001]:

$$f_c = 0.95 \cdot \tanh\left(100 \cdot S_n\right) \sqrt{\frac{1000 \cdot S_n}{1000 \cdot S_n + \varepsilon + 0.15\sigma_z}} \qquad (-) \qquad \{1\}$$

where f_s is snow cover fraction [*Uppala et al.*], S_n is the SWE, σ_z is standard deviation of subgrid orography (based on the 250m SRTM DEM) and ε is a very small number to avoid division by zero for totally flat and snow-free gridcells.

The glaciated regions in this part of the Himalaya can be defined as summer-accumulation types, with synchronous melt and accumulation periods during the summer monsoon [*Thayyen and Gergan*, 2010]. Figure 2 shows the distribution and occurrence of snow cover over the Ganges part of the Himalayas. Snow cover is more seasonably variable in the western part of the basin, whereas the eastern part is either hardly or permanently snow-covered. To the North-East rain shadowing effect of the mountain ranges leads to hardly any snow on the northern side, which is part of the Tibetan plateau.

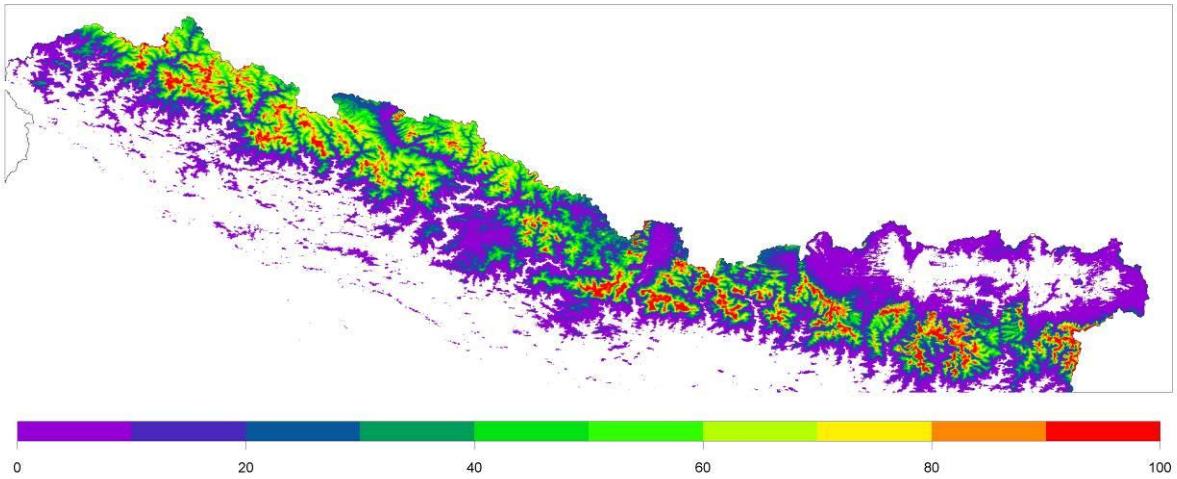

Figure 2. Occurrence of snow (in % of 8-day periods in a year) in the Ganges part of the Himalayas derived from MODIS (MOD10A2) 8-day aggregated snow cover product for the period 2001-2010

Figure 3 shows MODIS and modeled yearly snow cover dynamics over the whole basin. Snow cover starts to build up in August and September during the monsoon period, reaches its peak in February and then declines again till June. The average of yearly maximum snow cover of the whole basin, as derived from MODIS images, is 10.0% (STD 1.7) for the years 2001-2010. The average of yearly minimum snow cover is 1.2% (STD 0.9). Snow cover simulated by VIC corresponds very well to the measurements in terms of magnitude and seasonal pattern. With its 25 elevation bands, VIC calculates permanent snow cover in many grid cells along the Himalaya. LPJmL is slightly delayed in terms of seasonal pattern, but estimates decrease and increase and magnitude well. In JULES, build-up of snow cover is delayed till January-February and lower than measured. In models without elevation bands (JULES and LPJmL), snow cover or SWE has almost completely vanished mid-summer, with exception of two gridcells with high average elevation.

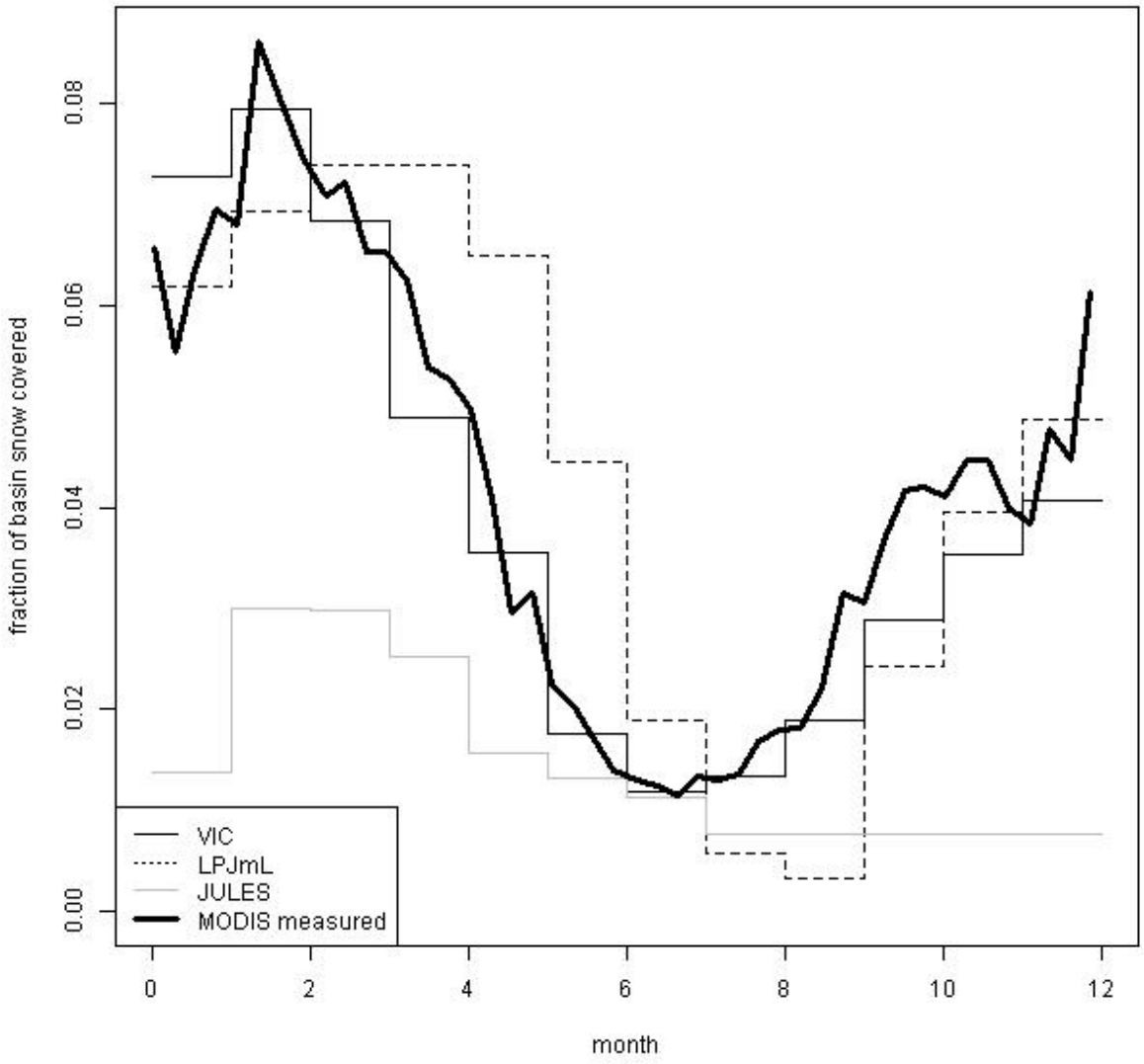

Figure 3.. Fraction of snow cover in the Ganges basin derived from MODIS MOD10A2 data (averaged over 2001-2010) and for the various models (using equation 2 based on Rousch et al., [2001] to convert modeled SWE to snow cover in LPJmL and JULES) for 1971-2000.

3.2 Discharge validation

For all stations the models show a monsoon influenced discharge pattern with discharge peaking in July-August. For the western Karnali catchment (Chisipani station) and central Narayani catchment (Devghat station) all models correctly model rise, height and decline of the discharge peak.

For the eastern subcatchment, Arun above Turkeghat, all models clearly overestimate runoff. Most likely this is caused by overestimation in WFD precipitation input data in the upper Arun catchment, on the dry Tibetan plateau. WFD precipitation appears high by comparison with APHRODITE and another data source, TRMM [*Bookhagen and Burbank*, 2010]; WFD precipitation is an order of magnitude greater than respective APHRODITE/TRMM values.

Sparse station coverage of the Tibetan plateau may result in WFD data being over-influenced by higher precipitation on Himalayan slopes to the south. However, limited precipitation makes the Arun catchment atypical; snowmelt contributes only a small percentage of runoff within the sub-catchment itself and the Ganges basin as a whole.
Discharges at Farakka (not shown) are overestimated by all models (37% to 82%), which can for a large part be explained by withdrawals for irrigation, which are not accounted for in the current model set-up. For the upstream station at Tehri (not shown) only data for 2000 till 2004 were available, which is largely outside the modeled period. Both maximum monthly average and mean monthly average discharge are overestimated by all models (16% to 127%). The upstream area of TERI is only covered by one gridcell in the models, which makes comparison sensitive to schematization and input biases.

References

Arnold, J. G., and N. Fohrer (2005), SWAT2000: current capabilities and research opportunities in applied watershed modelling, Hydrological Processes, 19(3), 563-572.
Batjes, N. H., 1995: A homogenized soil data file for global environmental research: A subset of FAO, ISRIC and NCRS profiles. *International Soil Reference and Information Centre (ISRIC) Technical Report* 95/10, 50 pp.
Best, M. J., et al. (2011), The Joint UK Land Environment Simulator (JULES), Model description – Part 1: Energy and water fluxes, *GeoScientific Model Development*, *4*(1), 595-640.
Clark, D. B., et al. (2011), The Joint UK Land Environment Simulator (JULES), Model description - Part 2: Carbon fluxes and vegetation, *GeoScientific Model Development*, *4*(1), 641-688.
FAO (1991), The digitized Soil map of the world , version 1.0. Food and Agriculture Organization of the United Nations, Rome.
FAO (1995), The digital soil map of the world, version 3.5. Food and Agriculture Organization of the United Nations, Rome.
FAO/IIASA/ISRIC/ISS-CAS/JRC (2009), Harmonized World Soil Database, version 1.1. Food and Agriculture Organization of the United Nations, Rome, Italy and IIASA, Laxenburg, Austria.
Gerten, D., S. Schaphoff, U. Haberlandt, W. Lucht, and S. Sitch (2004), Terrestrial vegetation and water balance - Hydrological evaluation of a dynamic global vegetation model, *Journal of Hydrology*, *286*(1-4), 249-270.
Gosain, A. K., S. Rao, and D. Basuray (2006), Climate change impact assessment on hydrology of Indian river basins, *Current Science*, *90*(3), 346-353.
Haddeland, I., et al. (2011), Multimodel Estimate of the Global Terrestrial Water Balance: Setup and First Results, *Journal of Hydrometeorology*, *12*(5), 869-884.
Hall, D. K., G. A. Riggs, and V. V. Salomonson (2006), MODIS/Terra Snow Cover 8-day L3 Global 500m Grid V005, jan 2000 - present, updated weekly, edited, National Snow and Ice Data Center, Boulder, Colorado USA.
Hansen, M. C., R. S. DeFries, J. R. G. Townshend, and R. Sohlberg (2000), Global land cover classification at 1 km spatial resolution using a classification tree approach. *International Journal of Remote Sensing*, 21, 1331–1364.

Liang, X., D. P. Lettenmaier, E. F. Wood, and S. J. Burges (1994), A Simple hydrologically Based Model of Land Surface Water and Energy Fluxes for GSMs, *Journal of Geophysical Research*, *99*(D7), 415-428.
Parajka, J., and G. Blöschl (2006), Validation of MODIS snow cover images over Austria, *Hydrology and Earth System Sciences*, *10*(5), 679-689.
Ramankutty, N., A. T. Evan, C. Monfreda, and J. A. Foley (2008), Farming the planet: 1. Geographic distribution of global agricultural lands in the year 2000, *Global Biogeochemical Cycles*, 22(1).
Roesch, A., M. Wild, H. Gilgen, and A. Ohmura (2001), A new snow cover fraction parametrization for the ECHAM4 GCM, *Climate Dynamics*, *17*(12), 933-946.
Rost, S., D. Gerten, A. Bondeau, W. Lucht, J. Rohwer, and S. Schaphoff (2008), Agricultural green and blue water consumption and its influence on the global water system, *Water Resources Research*, *44*(9), W09405.
Thayyen, R. J., and J. T. Gergan (2010), Role of glaciers in watershed hydrology: a preliminary study of a "Himalayan catchment", *The Cryosphere*, *4*, 115-128.
USGS, Global Land Cover Characteristics (version 2).
http://edc2.usgs.gov/glcc/globdoc2_0.php
van Zyl, J. J. (2001), The Shuttle Radar Topography Mission (SRTM): a breakthrough in remote sensing of topography, Acta Astronautica, 48(5-12), 559-565.
Weedon, G. P., S. Gomes, P. Viterbo, H. Österle, J. C. Adam, N. Bellouin, O. Boucher, and M. Best (2010), The WATCH forcing data 1958-2001: a meteorological forcing dataset for land surface- and hydrological-models. *WATCH Technical Report*.
Yatagai, A., O. Arakawa, K. Kamiguchi, H. Kawamoto, M. I. Nodzu, and A. Hamada (2009), A 44-year daily gridded precipitation dataset for Asia based on a dense network of rain gauges, *SOLA*, *5*, 137-140.